Data Collection	ATLAS DR3
Release Number	3
Data Provider	T Shanks
Date	<3.3.2017>

Authors: T Shanks[1], B. Chehade[1], NJG Cross[2], E Gonzalez-Solares[3], MJ Irwin[3], N Metcalfe[1] & MA Read[2]
[1]*Physics Department, University of Durham, South Road, Durham, DH1 3LE, UK*
[2]*Institute for Astronomy, Univ. of Edinburgh, Blackford Hill, Edinburgh EH9 3HJ, UK*
[3]*Institute of Astronomy, Univ. of Cambridge, Madingley Road, Cambridge, CB3 0HA, UK*

Abstract

The data being released are the VLT Survey Telescope (VST) ATLAS stacked reduced images and associated source lists taken from the start of observations by VST in August 2011, through to end September 2014 under ESO id 177.A-3011. Basic data reduction was done at the Cambridge Astronomical Surveys Unit (CASU). The passbands covered are the SDSS *u,g,r,i,z* bands reaching approximately the same depth (*r~22*) as the SDSS survey in the Northern Hemisphere. Seeing is specified to be between 1-1.4arcsec. The total sky coverage in DR3 is ~3700deg^2 of sky, out of the target of ~4700deg^2 in *i,z* and ~3000deg^2 out of ~4000deg^2 in *u,g,r*. Each ATLAS tile comprises a stacked pawprint composed of 2 pawprints offset by 25 arcsec in X and 85 arcsec in Y which takes out most of the inter-chip gaps between the 32 OmegaCAM CCDs. There are also 2arcmin overlaps in both RA and Dec between tiles to allow cross-calibration in the final data release. The ATLAS survey is particularly aimed at survey cosmology but can be exploited for many other branches of extragalactic and Galactic astronomy. Its wide wavelength coverage from the *u* to the *z* bands complements the VISTA Hemisphere and VIKING Surveys in the *YJHK* bands. A full description of the ATLAS survey is given by Shanks et al (2015, MNRAS, 451, 4238). DR3 is an "incremental" release for CASU images and source lists but a "superseding" release for bandmerged source lists from the Wide Field Astronomy Unit (WFAU) at Edinburgh.

Overview of Observations

Table 1 summarises the basic characteristics of the ATLAS DR3 data release:

Table 1 – Basic VST ATLAS DR3 summary

	u	g	r	i	z
Exposure (s)	2x60s	2x50s	2x45s	2x45s	2x45s
No. of Tiles	2470 (301)	3212 (761)	3316 (670)	3936 (753)	4021 (856)
No. of Stacked Pawprints	3215 (496)	3709 (862)	3930 (740)	5656 (1191)	6058 (1426)
~Area (deg^2)	2308	3001	3099	3687	3757
Median Mag Lim.	22.01(21.86)	23.16(23.25)	22.70(22.70)	22.02(22.03)	20.89(20.90)
Median Sky Bri.	22.43(22.42)	21.96(22.03)	20.96(21.05)	19.84(19.84)	18.88(18.88)
20mag e$^-$/s	29	177	160	101	29
Median Seeing "	1.05 (1.25)	0.95 (1.01)	0.90 (0.96)	0.81 (0.78)	0.84 (0.83)

Notes: Rows (2,3,5,6,8): The first number is DR2+DR3. In brackets are DR3 (CASU) only. The number of stacked pawprints is more than the number of tiles covered because of the inclusion of repeated observations. Rows(5,6,8) Medians for ESO Grades A,B. Row (5): Median 5σ AB point source magnitude limit in 2arcsec aperture for ATLAS DR3. Row (6): Median sky brightness in AB mags/arscec^2. Row (7): fluxes for AB 20mag point sources, normalized to airmass 1.3. All magnitude limits and sky brightnesses are in a system close to SDSS AB.

These exposure times are longer than the ~55s of SDSS to take into account the 0.21arcsec pixels of VST OmegaCam compared to the 0.4 arcsec SDSS pixels and slightly brighter skies for ATLAS in *i* and *z* and produces approximately similar S/N as SDSS in all bands. Note that ATLAS OBs are generally composed of a concatenation of 17 tiles in a given band, taken in fixed Declination strips in the direction of increasing RA. The *ugr* images are taken in dark time and the *iz* images are taken in grey/bright time.

Images and source lists for all ESO Grades are being supplied. The specified survey quality is limited to ESO Grade A, B and occasionally C, in cases where only a single tile in a 17 tile concatenation was at C grade. Otherwise C and D grade tiles either have been or will be repeated. But all available data are being supplied in this release, partly because ~4% of images have no ESO grades available. This causes the total number of DR3 stacked pawprints (4715) to be larger than the total number of tiles observed (3341) (see also Table 1). The TL_RA and TL_DEC header keywords are identical for all data belonging to the same tile. The most recent stacked pawprint of a given tile and filter is generally the one with OBSTATUS = Completed. Including single pawprints + confidence maps + source lists, the CASU component of DR3 comprises 14145 files. The WFAU DR3 component comprises 3992 bandmerged catalogue files plus one metadata file. Fig. 1 below shows the ATLAS coverage at 30/09/14 on which the DR2+DR3 CASU and DR3 WFAU releases are based. A different map applies to each band.

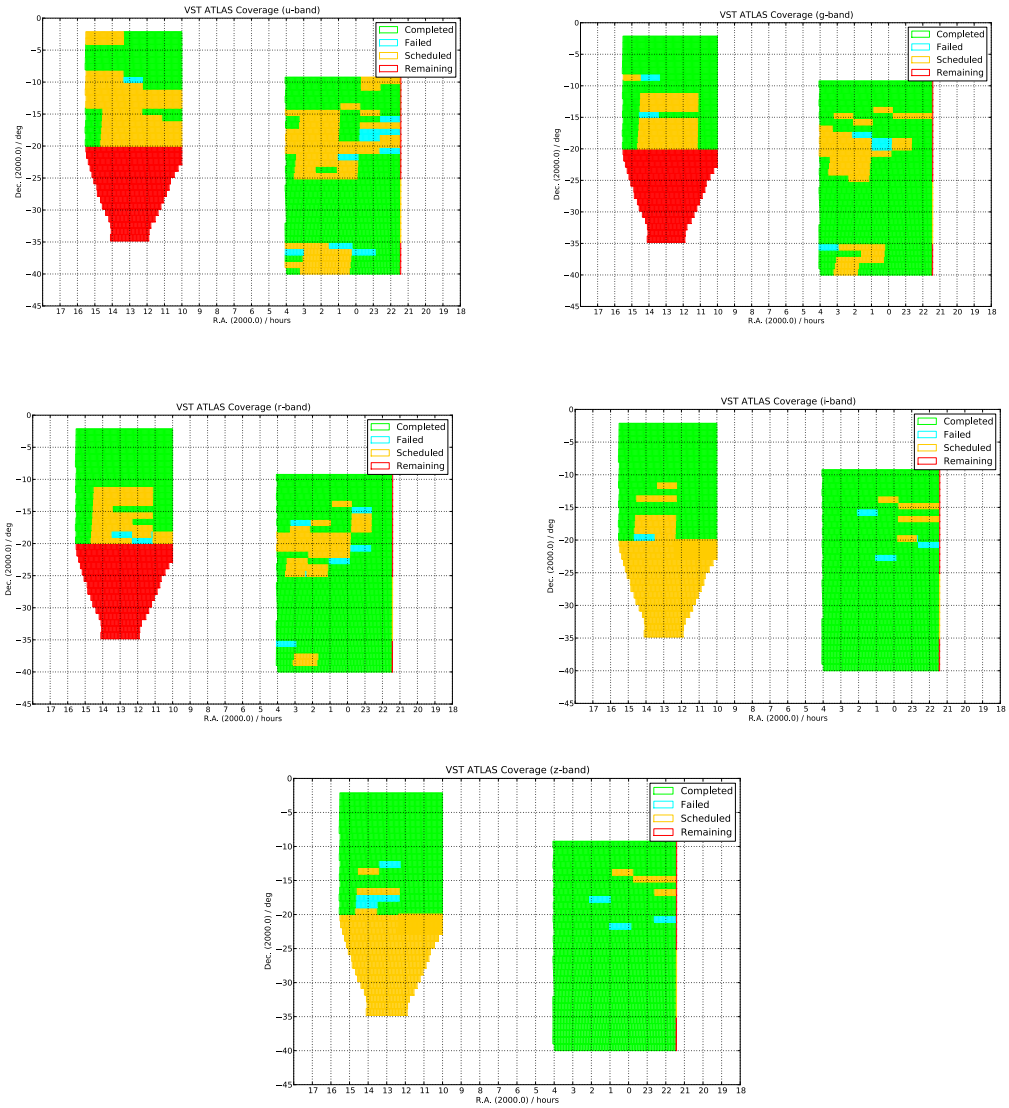

Fig.1. VST ATLAS coverage of tiles in the DR2+DR3 data releases. From top left, ugriz bands. Green means tiles successfully completed by end of September 2014. Blue means failed, yellow means OB submitted and red means no OB submitted by this same date. DR2+DR3 includes most of the tiles marked green and blue.

Release Content

The CASU imaging data comprises the combination of the two individual pawprint images which goes to make an ATLAS stacked pawprint in each tile. Each file is in a multi-extension fits (MEF) format with an extension for each of the 32 OmegaCam CCDs in the stacked pawprint. Individual CCDs originally contained 2048x4096 pixels and the stacked pawprint extensions contain approximately 2165x4500 pixels to cover the two 25"x85"offset CCDs that make up each extension in a stack. Along with the imaging data, we are also releasing statistical confidence maps in the same format. The seeing is specified to be <1.4 arcsec FWHM and the distributions by passband are shown in Fig. 2. The distribution of limiting magnitudes at the 5σ detection level by passband is shown in Fig. 3. DR3 comprises a total of 14145 CASU data files (including stacked pawprints + confidence maps + source lists) occupying a total of ~2Tb uncompressed or ~1.3Tb in its default Rice compression. The total area covered by DR2+DR3 is ~3000-4000 deg^2. The 2-pointing dither leaves 14 small (2x80x20arcsec^2) holes amounting to 1/3% of the total area. Since different bands are observed at different times some tiles have currently only partial passband coverage. Also included in DR3 are 3993 bandmerged source lists from WFAU comprising ~106x10^6 data columns (see Data Format section below). The WFAU DR3 source lists cover all tiles taken up to 30/9/14 whereas CASU DR3 imaging and source lists cover data taken between 1/10/13-30/9/14.

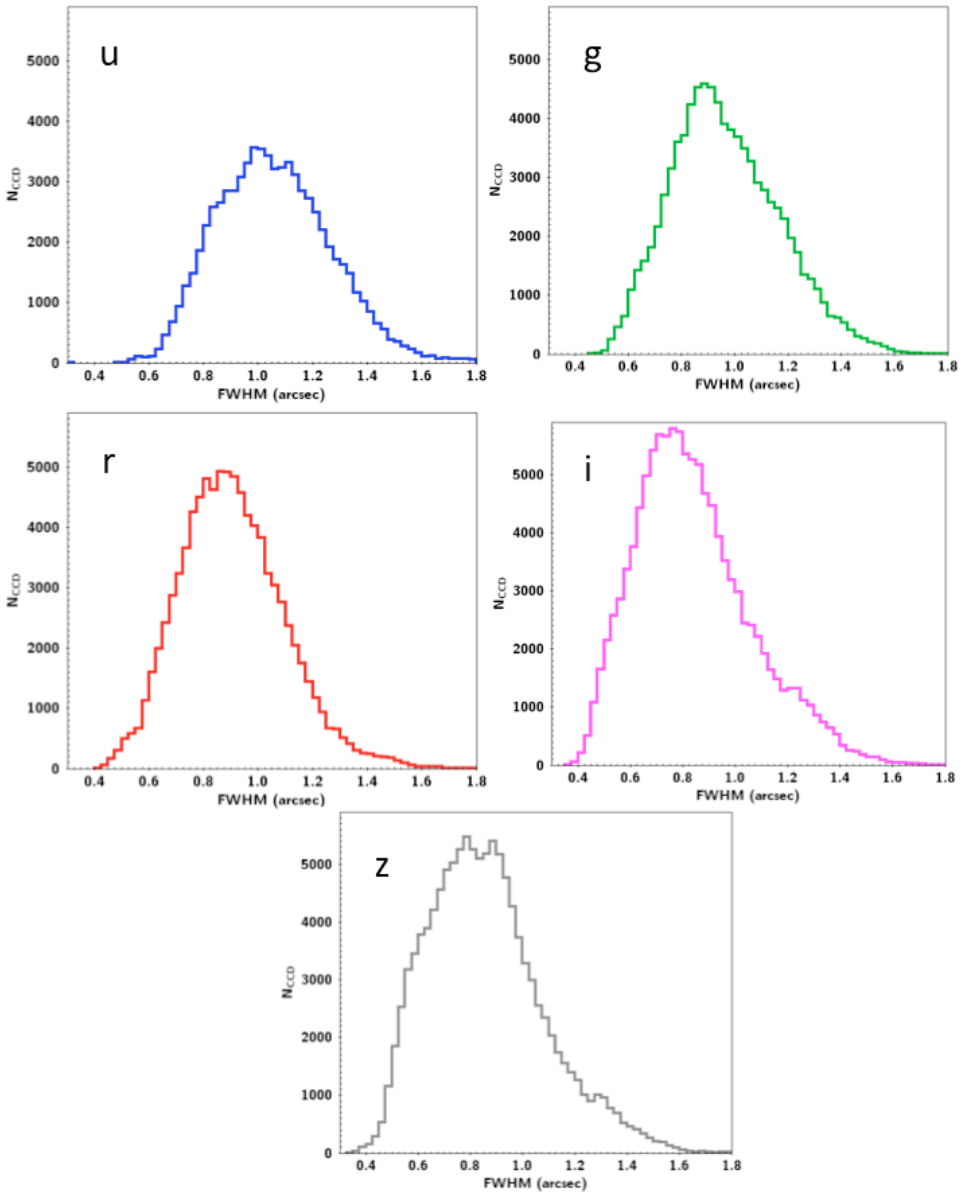

Fig. 2. Seeing (FWHM) distributions from ATLAS data release DR2+DR3 for ESO A and B grades.

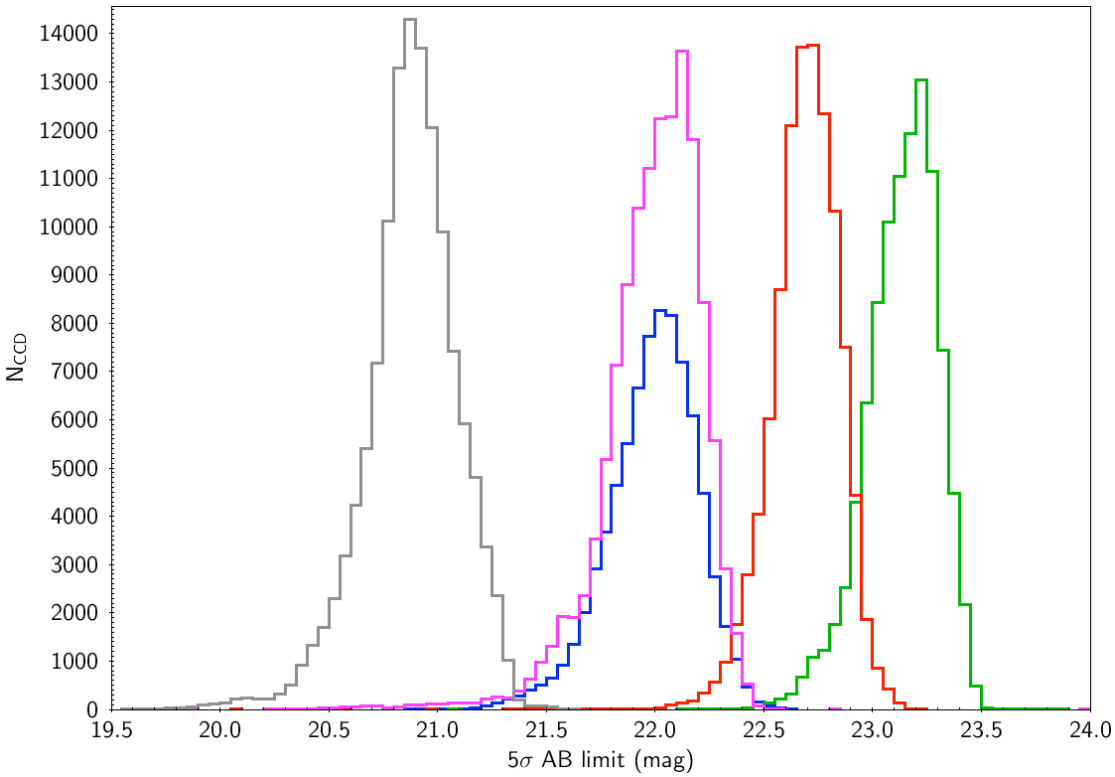

Fig. 3. ATLAS 5σ AB magnitude limit distributions for DR2+DR3 point sources in u (blue), g (green), r (red), i (purple) and z (grey) for A and B grade tiles. The median magnitude limits are given in Table 1.

The CASU source list data covers the same pixel areas as the stacked pawprints (see above). The derived object source lists are also stored as multi-extension FITS files using FITS binary tables, one for each image extension with the primary header unit containing the telescope and observation-specific information. The source list extension headers contain a copy of the relevant detector-specific information. Each detected object has an attached set of descriptors, forming the columns of the binary table and summarising derived position, shape and intensity information. During further processing stages ancillary information such as the sky properties, seeing and so on are derived from the source lists and stored in the FITS headers attached to each source list extension. All derived parameters are stored as floating point numbers. A full description of the source list columns is given at
http://apm49.ast.cam.ac.uk/surveys-projects/vst/technical/catalogue-generation

Release Notes

Astrometric calibration is via the numerous unsaturated 2MASS point sources available in each tile. By stacking residuals from a series of standard Tangent Plane astrometric fits based on 2MASS we can see (as in the example in Fig. 4 below) that there are no significant astrometric distortions over the whole field of view. The individual detector astrometric solutions achieve rms accuracies of around 70-80mas per star - generally dominated by rms errors in 2MASS stars. Even at high Galactic latitudes there are sufficient calibrators to give systematic residuals at the ~25mas level per detector. The global systematics from stacking multiple solutions are better than this as can be seen in Fig. 4. A Tangent Plane projection (TAN) is being used for all data products.

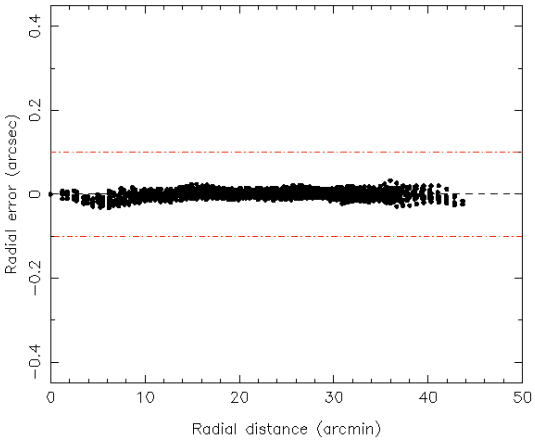

Fig. 4. Astrometric VST-2MASS residuals for stars as a function of distance from tile centre.

The original ATLAS(ESO) photometric calibration of each pointing is based on the limited number of standard fields observed by VST each night. This calibration was in a VST Vega-like system, but, as the average standard star SED and the detector response drops rapidly in the UV, it would be surprising if there were not issues in at least the *u*-band calibration. Note that these zero-points are still based on the original source lists rather than the illumination-correction fixed source lists (see below). An improved AB calibration for DR2+DR3 based on the AAVSO Photometric All-Sky Survey (APASS-http://www.aavso.org/apass) is described in the Data Reduction and Calibration section below.

In addition there are available a few extra calibration OBs taken with shorter exposures in photometric conditions to give an independent photometric calibration of tiles within the ATLAS footprint of the *ugriz* sequences from http://www-star.fnal.gov/Southern-ugriz/www/Fieldindex.html . In the overall header there is the keyword HIERARCH ESO OBS NAME which contains the OB name. This will include the word "standards" if it is one of the short exposure standard star fields. In total, twelve of these fields lie within the ATLAS region, split evenly between our SGC and NGC areas. Ultimately these can be used along with the 2arcmin tile overlaps and external surveys such as - http://www.aavso.org/apass) to anchor the global calibration in the final ATLAS release.

Also included are *ugriz* images and source lists centred on the William Herschel Deep Field at $00^{h}22^{m}33.3^{s}$ +00°20'57" (J2000) and overlapping SDSS Stripe 82. These deeper data were used to test the ATLAS depth in the early stages of the survey and full details are given in Table 2 of Shanks et al (2015, MNRAS, 451, 4238). These files are identified in the headers by the OBJECT keyword being set to "ATLAS depth test".

There are a few other tiles included that are not in the ATLAS footprint. These are mainly observations taken in error at the telescope.

Data Reduction and Calibration

The data processing of the science products released in this data release comes from version 1.0 of the VST Data Flow System (VDFS) pipeline running at CASU, but unlike VPHAS did not require the additional use of the nebulosity filter prior to source extraction. Saturated stars can be automatically flagged post-processing according to user needs. The reflection artefacts around heavily saturated bright stars can generate spurious detections but the contamination is reduced if source lists are matched during band-merging. As specified in the Survey Management Plan, source lists for individual pawprints are supplied with no attempt to reject overlaps. Such a catalogue will be produced for the final, globally calibrated survey. The astrometric reference catalogue is 2MASS. The Vega photometric reference system currently is based on the *ugriz* standards specified by ESO, but the DR2 and DR3 ATLAS releases also include AB zeropoints based on science data matches with the APASS survey. The illumination correction is already made from a comparison of each month of data from all VST public surveys with the APASS survey. This correction has been applied to source list photometry but not to image pixels. (CASU have devel-

oped software to apply the illumination correction to image pixels. Since scattered light is also present in dark sky science images the optimum way to use this correction depends on the end-user requirements so this correction is not routinely applied to the stored images). Global calibration will be addressed in the final release. Stellar aperture corrections are supplied for each photometric aperture used in the source list and these can be used to estimate total fluxes or magnitudes for stars. PSF magnitudes will be produced for the final data release. Source fluxes in the binary tables are in ADUs and require corrections for aperture loss, airmass (relative to unity), and application of the appropriate magnitude zeropoint. The relevant information is supplied in the source list headers. No correction for Galactic extinction has been applied or supplied, in part because the correction is specific to the extinction model adopted.

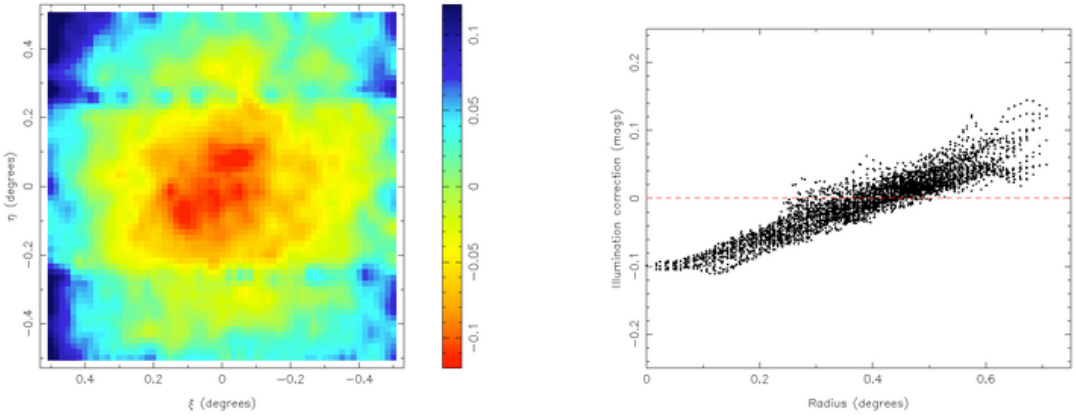

Fig 5. The illumination correction in the i-band as measured by residuals from APASS photometry. The released source lists have had the illumination correction applied based on source position in the image plane.

Data Quality

The astrometric calibration is uniform across the survey to an *rms* accuracy of 25mas relative to 2MASS. Indeed, various fields scattered across the ATLAS area have already been used as the basis for 2dF fibre observations with no astrometric problem. The main problem in the released images is a non-uniform photometric response across the field caused by the presence of scattered light in the VST flat-fields. with a pattern across the pawprint which typically looks like that shown in Fig. 5. The scattered light is made up of multiple components having different symmetries and scales causing effects ranging in scale from ten arcsec with x-y rectangular symmetry, e.g. due to scattering off masking strips of CCDs, to large fractions of the field due to radial concentration in the optics and to non-astronomical scattered light entering obliquely in flats. The illumination correction removes the dominant reproducible components of this effect in the source lists leaving the zeropoint across the field uniform to ~±0.003mag. (We note that after the recent VST baffling improvements, and particularly after January 2014, the size of the illumination correction required has dropped by more than a factor of two and in current data the range is approximately +/- 0.05 magnitudes). In addition, one detector, #82, otherwise known as CCD #10 in the MEF extensions, had a gain which intermittently varied by up to 0.5 mag until the video board replacement in June 2012; this may not always be taken out by the flatfield.

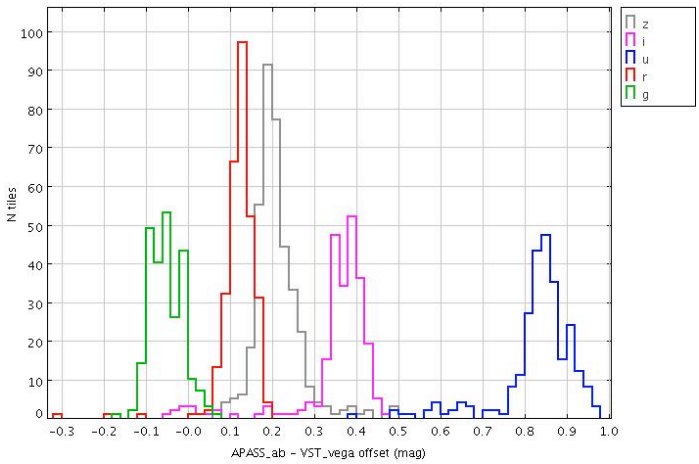

Fig. 6. The ugriz distributions of APASS AB-VST Vega offsets for m<16mag stars from ~240 tiles in the SGP GAMA region.

The original (ATLAS-ESO) magnitude zeropoint calibration and error (MAGZPT and MAGZRR in the header) was good to ±0.05mag between tiles across the survey, as estimated from a comparison with APASS m<16 stellar magnitudes (see Fig. 6). This zeropoint calibration applied in the (PHOTSYS=)Vega magnitude system across all filters and epochs. In this calibration, zeropoints of colour indices may thus be good to ~±0.07mag. Note that PHOTZP and PHOTZPER also refer to this original (PHOTSYS=)Vega magnitude system but the PHOTZP zeropoint now includes the effects of exposure time and airmass.

With DR2 and DR3 two new magnitude zeropoints are now available based on APASS stellar photometry to ~16mag. The APASS zeropoint (APASSZPT in the header) and its error (APASSZRR) is based on a comparison of APASS and ATLAS stars in the 13<m<16mag range within each stacked pawprint. The number of stars that contributed to each pawprint zeropoint is given by APASSNUM. The ATLAS-APASS nightly zeropoint and error (NIGHTZPT and NIGHTZRR in the header) is based on the average of all the APASS zeropoints measured on a given night in a particular passband. The number of APASS zeropoints that contributed to this nightly zeropoint is given by NIGHTNUM.

We estimate the accuracy of the ATLAS(APASS) nightly zeropoint from a comparison with SDSS in its 120deg^2 overlap area with ATLAS in the NGC. The ATLAS(APASS) - SDSS magnitude standard deviations are ±0.035, ±0.013, ±0.013, ±0.012 and ±0.055 mag in *ugriz*, in most bands a significant improvement over the ATLAS(ESO) - SDSS comparison (±0.045, ±0.027, ±0.037, ±0.035 and ±0.073 in *ugriz*). The ATLAS-APASS nightly zeropoint is therefore recommended for use in ATLAS DR2 and DR3.

Quality of magnitudes have been better checked for point sources than for galaxies. It may be possible to extend depth for galaxies by specific smoothing of image before source detection.

Contamination of the source list by spurious sources is at the <5% level down to the limiting magnitudes estimated in the headers. The source lists are estimated to be ~50% complete at the quoted 5σ limiting magnitudes.

Finally, in Fig. 7 we show for a science example, colour-colour diagrams for g<22.5 stars in one ATLAS tile as recently used to select quasars for the 2dF QSO Dark Energy Survey pilot at the Anglo-Australian Telescope (AAT).

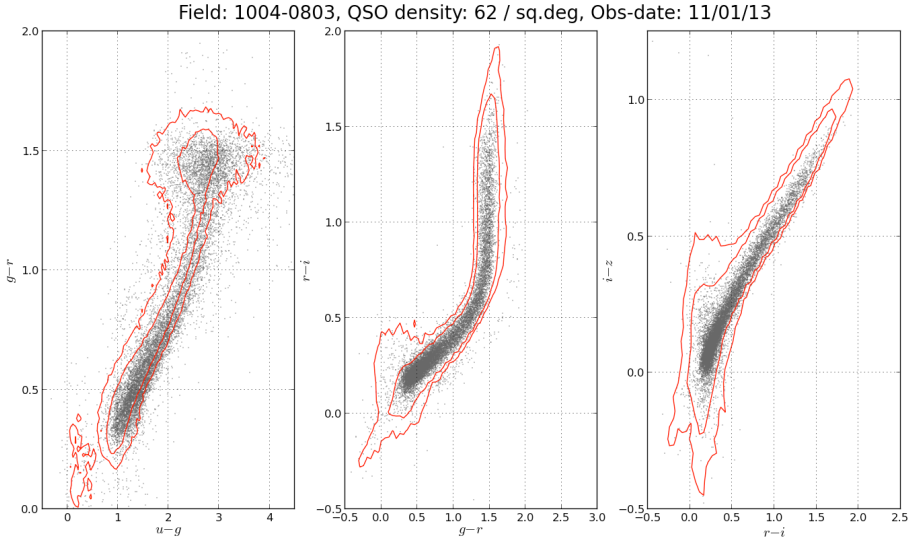

Fig. 7. ugr, gri and riz colour-colour diagrams for stellar objects to g~22.5 in an ATLAS tile as used to select QSO targets for AAT 2dF. The red contours are from SDSS selected stars for comparison.

Known issues

The illumination correction for scattered light in the flatfields has only been applied to source lists and not the image pixels. This problem will have to be addressed before attempting surface photometry of very large galaxies but even then the additive scattered light present in all images may preclude achieving reliable surface photometry at faint magnitudes.

We also note the occasional presence of pickup noise in some observations at the level of ±10ADU caused by guide/wavefront sensor readout happening at same time as science frame read-out. A similar pickup pattern occurs on all 32 detectors and is fixable in post-processing. This problem was (mostly) fixed by some modifications to control software in Autumn 2012.

Note that in observations taken in approximately the first 2 months of the survey, ie before 3/10/11, the 25 arcsec dither in X(~RA) between the two pawprints that make up the stacked pawprint was gradually reduced as each of the 17 tiles in a Group for a given RA range was observed, due to a VST technical problem. This means that the main CCD gaps in the Dec direction are not filled in as well as they should be in the stacked pawprint. Data taken after the above date were taken as concatenations and should be unaffected by this problem.

For source lists, the correct keyword values that characterise the observation at large (e.g. T/EXPTIME, MJD-OBS, TELESCOP etc) are to be taken from the primary header, and not from the extension header.

113 CASU source list files have PHOTZPERR = -1 indicating that no ESO standard calibration was available for these fields. In these cases a fixed standard ESO Vega zeropoint has been applied.

Previous Releases

DR1 was the first data release for VST ATLAS. DR1 was superseded by DR2. DR2 therefore improved on the data released in DR1 and included 94 new files for the DR1 period 8/11-9/12 as listed below. The main reason most were omitted was because they were ESO test data. Although "ATLAS depth test" usually appears in the header, this is a misnomer for these files since they were generally made as part of an ESO "Concatenation test" when ATLAS moved to use concatenations of observing blocks. But much of these data is good quality and so they were included in DR2. The other files listed below are either Survey data that was inadvertently missed out of DR1 or data that was taken in error outside the survey footprint.

o20110820_00087_st_cat.fits o20110820_00087_st.fits.fz ATLAS depth test -> Concatenation test
o20110820_00089_st_cat.fits o20110820_00089_st.fits.fz " "

o20110820_00091_st_cat.fits o20110820_00091_st.fits.fz " "
o20110820_00093_st_cat.fits o20110820_00093_st.fits.fz " "
o20110820_00095_st_cat.fits o20110820_00095_st.fits.fz " "
o20110820_00097_st_cat.fits o20110820_00097_st.fits.fz " "
o20110820_00099_st_cat.fits o20110820_00099_st.fits.fz " "
o20110820_00101_st_cat.fits o20110820_00101_st.fits.fz " "
o20110820_00103_st_cat.fits o20110820_00103_st.fits.fz " "
o20110820_00105_st_cat.fits o20110820_00105_st.fits.fz " "
o20110820_00107_st_cat.fits o20110820_00107_st.fits.fz " "
o20110820_00109_st_cat.fits o20110820_00109_st.fits.fz " "
o20110820_00111_st_cat.fits o20110820_00111_st.fits.fz " "
o20110820_00113_st_cat.fits o20110820_00113_st.fits.fz " "
o20110820_00115_st_cat.fits o20110820_00115_st.fits.fz " "
o20110820_00117_st_cat.fits o20110820_00117_st.fits.fz " "
o20110820_00119_st_cat.fits o20110820_00119_st.fits.fz " "
o20110821_00091_st_cat.fits o20110821_00091_st.fits.fz " "
o20110821_00093_st_cat.fits o20110821_00093_st.fits.fz " "
o20110821_00095_st_cat.fits o20110821_00095_st.fits.fz " "
o20110821_00097_st_cat.fits o20110821_00097_st.fits.fz " "
o20110821_00099_st_cat.fits o20110821_00099_st.fits.fz " "
o20110830_00029_st_cat.fits o20110830_00029_st.fits.fz RA, Dec outside survey area
o20110830_00031_st_cat.fits o20110830_00031_st.fits.fz "
o20110830_00033_st_cat.fits o20110830_00033_st.fits.fz "
o20110830_00035_st_cat.fits o20110830_00035_st.fits.fz "
o20110830_00037_st_cat.fits o20110830_00037_st.fits.fz "
o20110831_00022_st_cat.fits o20110831_00022_st.fits.fz ATLAS depth test -> Concatenation test
o20110831_00024_st_cat.fits o20110831_00024_st.fits.fz " "
o20110831_00026_st_cat.fits o20110831_00026_st.fits.fz " "
o20110831_00028_st_cat.fits o20110831_00028_st.fits.fz " "
o20110831_00030_st_cat.fits o20110831_00030_st.fits.fz " "
o20110831_00032_st_cat.fits o20110831_00032_st.fits.fz " "
o20110831_00034_st_cat.fits o20110831_00034_st.fits.fz " "
o20110831_00036_st_cat.fits o20110831_00036_st.fits.fz " "
o20110831_00038_st_cat.fits o20110831_00038_st.fits.fz " "
o20110831_00040_st_cat.fits o20110831_00040_st.fits.fz " "
o20110831_00042_st_cat.fits o20110831_00042_st.fits.fz " "
o20110831_00044_st_cat.fits o20110831_00044_st.fits.fz " "
o20110831_00046_st_cat.fits o20110831_00046_st.fits.fz " "
o20110831_00048_st_cat.fits o20110831_00048_st.fits.fz " "
o20110831_00050_st_cat.fits o20110831_00050_st.fits.fz " "
o20110831_00052_st_cat.fits o20110831_00052_st.fits.fz " "
o20110831_00054_st_cat.fits o20110831_00054_st.fits.fz " "
o20110924_00166_st_cat.fits o20110924_00166_st.fits.fz ATLAS Survey data
o20110929_00042_st_cat.fits o20110929_00042_st.fits.fz Subsequently re-observed
o20111119_00042_st_cat.fits o20111119_00042_st.fits.fz ATLAS Survey data

The 6 files following were included in DR1 and are now deprecated/dropped from DR2 because they represent observations whose exposure was interrupted:
o20110904_00013_st_cat.fits o20110904_00013_st.fits.fz
o20110907_00005_st_cat.fits o20110907_00005_st.fits.fz
o20110904_00066_st_cat.fits o20110904_00066_st.fits.fz

The DR3 release of CASU imaging and source lists now delivers entirely new data covering observations made between 1/10/13 to 30/9/14. These data have therefore to be used alongside the DR2 CASU data, covering the period from survey start to 30/9/14, to achieve the sky coverage shown in Fig. 1.

On the other hand, the DR3 band-merged source lists from WFAU cover all observations taken

from the survey start to 30/9/14 and so supersede the ATLAS data released from WFAU in DR2. Note that the following WFAU source lists appear in DR2 but not in DR3 because a new band has become available but with one or more detector extensions deprecated which means a complete band-merged file is unable to be included in DR3:

atlas_er2_00h17-014d41_ugriz_finalSourceCat_1951.fits
atlas_er2_00h25-014d41_ugriz_finalSourceCat_1953.fits
atlas_er2_00h40-017d39_ugriz_finalSourceCat_1707.fits
atlas_er2_00h55-015d40_ugriz_finalSourceCat_1856.fits
atlas_er2_01h18-023d36_ugriz_finalSourceCat_1400.fits
atlas_er2_02h01-027d35_ugriz_finalSourceCat_1071.fits
atlas_er2_03h46-024d36_ugriz_finalSourceCat_1302.fits
atlas_er2_03h47-021d37_ugriz_finalSourceCat_1528.fits
atlas_er2_11h11-015d31_ugriz_finalSourceCat_1898.fits
atlas_er2_11h15-015d31_ugriz_finalSourceCat_1899.fits
atlas_er2_11h19-015d31_ugriz_finalSourceCat_1900.fits
atlas_er2_11h23-015d31_ugriz_finalSourceCat_1901.fits
atlas_er2_11h27-015d31_ugriz_finalSourceCat_1902.fits
atlas_er2_11h31-015d31_ugriz_finalSourceCat_1903.fits
atlas_er2_11h39-015d31_ugriz_finalSourceCat_1905.fits
atlas_er2_11h44-015d31_ugriz_finalSourceCat_1906.fits
atlas_er2_11h48-015d31_ugriz_finalSourceCat_1907.fits
atlas_er2_11h52-015d31_ugriz_finalSourceCat_1908.fits
atlas_er2_12h00-015d31_ugriz_finalSourceCat_1910.fits
atlas_er2_12h08-015d31_ugriz_finalSourceCat_1912.fits

Data Format

Files Types

The CASU image files are in multi-extension FITS (MEF) format with an extension for each of the 32 CCDs in each stack**.** The CASU derived object source lists are also stored in multi-extension FITS files as FITS binary tables, one extension for each image extension with the primary header unit containing the telescope and observation-specific information. The source list extension headers contain a copy of the relevant detector-specific information.

Both CASU images and source list filenames are in the form o20110914_00092 where the night of observation is followed by the ESO VST nightly run number. The suffix _st indicates that the image or source list is based on a stacked pawprint. A suffix _cat indicates that the file corresponds to a source list. A suffix _conf indicates that the file contains the statistical confidence map for the tile. The file type fits.fz indicates Rice compressed FITS file and these can be de-compressed using e.g. CFITSIO *funpack*.

The DR3 release again contains bandmerged source lists produced by the Wide Field Astronomy Unit (WFAU), Edinburgh. These files combine a subset of the parameters as supplied in the CASU lists but now with magnitudes calculated from fluxes and observations merged so that colour indices are provided. Additional parameters include extinction coefficients, merged classification statistics and error bit flagging. The magnitudes are computed based on the ATLAS(APASS) nightly zeropoints described above. The data files are based on framesets formed by merging catalogues from individual detectors. Filenames are of the form atlas_er3_23h53-024d36_ugriz_fsc_NNNN.fits where NNNN is just an integer framesetID that represents the combination of observations used in the merger.

Source list columns

A full description of the CASU source list columns is given at
http://apm49.ast.cam.ac.uk/surveys-projects/vst/technical/catalogue-generation

Full descriptions of the WFAU bandmerged catalogue columns is given in Appendix 1. There are 160 columns per source. Flags uClass, gClass,... refer to the most probable morphological classification in each band where -1=stellar, +1=non-stellar, 0=noise and -2=borderline stellar. For description of other flags see the above link and http://osa.roe.ac.uk/ATLASDR2/ATLASDR2_TABLE_atlasSourceSchema.

Each WFAU file is the catalogue of a "tile". But the source merging works only at the CCD detector/extension level. So what is supplied are really pseudo tile based merged catalogues from concatenating the 32 individual catalogues. The merging/seaming therefore still suffers from the CCD edge effects when there are large offsets between the filters so similar caveats apply as discussed at http://osa.roe.ac.uk/ - Known Issues

You can partly avoid duplicates using (priorsec=0 or priorsec=framesetid) or indeed use the PRIMARY_SOURCE keyword. However, while the latter will remove duplicates it will also have the effect of occasionally causing sources to miss measurements in some bands.

Acknowledgements

Please use the following statement in your articles when using these data:

Based on data products from observations made with ESO Telescopes at the La Silla Paranal Observatory under program ID *177.A-3011(A,B,C,D,E,F,G,H,I,J)*(see Shanks et al 2015, MNRAS, 451, 4238).

Appendix 1: WFAU bandmerged catalogue column descriptions

Column: Name; FITS data type; Description

1 : IAUNAME; 35A; IAU Name (not unique)
2 : sourceID; K; UID (unique over entire OSA via programme ID prefix) of this merged detection as assigned by merge algorithm
3 : cuEventID; J; UID of curation event giving rise to this record
4 : frameSetID; K; UID of the set of frames that this merged source comes from
5 : ra2000; D; Celestial Right Ascension
6 : dec2000; D; Celestial Declination
7 : l; D; Galactic longitude
8 : b; D; Galactic latitude
9 : lambda; D; SDSS system spherical co-ordinate 1
10 : eta; D; SDSS system spherical co-ordinate 2
11 : priOrSec; K; Seam code for a unique (=0) or duplicated (!=0) source (eg. flags overlap duplicates).
12 : umgPnt; E; Point source colour U-G (using aperMag3)
13 : umgPntErr; E; Error on point source colour U-G
14 : gmrPnt; E; Point source colour G-R (using aperMag3)
15 : gmrPntErr; E; Error on point source colour G-R
16 : rmiPnt; E; Point source colour R-I (using aperMag3)
17 : rmiPntErr; E; Error on point source colour R-I
18 : imzPnt; E; Point source colour I-Z (using aperMag3)
19 : imzPntErr; E; Error on point source colour I-Z
20 : umgExt; E; Extended source colour U-G (using aperMagNoAperCorr3)
21 : umgExtErr; E; Error on extended source colour U-G
22 : gmrExt; E; Extended source colour G-R (using aperMagNoAperCorr3)
23 : gmrExtErr; E; Error on extended source colour G-R
24 : rmiExt; E; Extended source colour R-I (using aperMagNoAperCorr3)
25 : rmiExtErr; E; Error on extended source colour R-I

26 : imzExt; E; Extended source colour I-Z (using aperMagNoAperCorr3)
27 : imzExtErr; E; Error on extended source colour I-Z
28 : mergedClassStat; E; Merged N(0,1) stellarness-of-profile statistic
29 : mergedClass; I; Class flag from available measurements (1|0|-1|-2|-3|-9=galaxy|noise|stellar|probableStar|probableGalaxy|saturated)
30 : pStar; E; Probability that the source is a star
31 : pGalaxy; E; Probability that the source is a galaxy
32 : pNoise; E; Probability that the source is noise
33 : pSaturated; E; Probability that the source is saturated
34 : eBV; E; The galactic dust extinction value measured from the Schlegel, Finkbeiner & Davis (1998) maps. This uses the correction given in Bonifacio, Monai & Beers (2000). This correction reduces the extinction value in regions of high extinction (E(B-V)>0.1)
35 : aU; E; The galactic extinction correction in the U band for extragalactic objects
36 : aG; E; The galactic extinction correction in the G band for extragalactic objects
37 : aR; E; The galactic extinction correction in the R band for extragalactic objects
38 : aI; E; The galactic extinction correction in the I band for extragalactic objects
39 : aZ; E; The galactic extinction correction in the Z band for extragalactic objects
40 : uMjd; D; The mean Modified Julian Day of each detection
41 : uPetroMag; E; Extended source U mag (Petrosian)
42 : uPetroMagErr; E; Error in extended source U mag (Petrosian)
43 : uAperMag3; E; Default point source U aperture corrected mag (2.0 arcsec aperture diameter)
44 : uAperMag3Err; E; Error in default point/extended source U mag (2.0 arcsec aperture diameter)
45 : uAperMag4; E; Point source U aperture corrected mag (2.8 arcsec aperture diameter)
46 : uAperMag4Err; E; Error in point/extended source U mag (2.8 arcsec aperture diameter)
47 : uAperMag6; E; Point source U aperture corrected mag (5.7 arcsec aperture diameter)
48 : uAperMag6Err; E; Error in point/extended source U mag (5.7 arcsec aperture diameter)
49 : uAperMagNoAperCorr3; E; Default extended source U aperture mag (2.0 arcsec aperture diameter)
50 : uAperMagNoAperCorr4; E; Extended source U aperture mag (2.8 arcsec aperture diameter)
51 : uAperMagNoAperCorr6; E; Extended source U aperture mag (5.7 arcsec aperture diameter)
52 : uHlCorSMjRadAs; E; Seeing corrected half-light, semi-major axis in U band
53 : uGausig; E; RMS of axes of ellipse fit in U
54 : uEll; E; 1-b/a, where a/b=semi-major/minor axes in U
55 : uPA; E; ellipse fit celestial orientation in U
56 : uErrBits; J; processing warning/error bitwise flags in U
57 : uAverageConf; E; average confidence in 2 arcsec diameter default aperture (aper3) U
58 : uClass; I; discrete image classification flag in U
59 : uClassStat; E; N(0,1) stellarness-of-profile statistic in U
60 : uppErrBits; J; additional WFAU post-processing error bits in U
61 : uSeqNum; J; the running number of the U detection
62 : uXi; E; Offset of U detection from master position (+east/-west)
63 : uEta; E; Offset of U detection from master position (+north/-south)
64 : gMjd; D; The mean Modified Julian Day of each detection
65 : gPetroMag; E; Extended source G mag (Petrosian)
66 : gPetroMagErr; E; Error in extended source G mag (Petrosian)
67 : gAperMag3; E; Default point source G aperture corrected mag (2.0 arcsec aperture diameter)
68 : gAperMag3Err; E; Error in default point/extended source G mag (2.0 arcsec aperture diameter)
69 : gAperMag4; E; Point source G aperture corrected mag (2.8 arcsec aperture diameter)
70 : gAperMag4Err; E; Error in point/extended source G mag (2.8 arcsec aperture diameter)
71 : gAperMag6; E; Point source G aperture corrected mag (5.7 arcsec aperture diameter)
72 : gAperMag6Err; E; Error in point/extended source G mag (5.7 arcsec aperture diameter)
73 : gAperMagNoAperCorr3; E; Default extended source G aperture mag (2.0 arcsec aperture diameter)
74 : gAperMagNoAperCorr4; E; Extended source G aperture mag (2.8 arcsec aperture diameter)
75 : gAperMagNoAperCorr6; E; Extended source G aperture mag (5.7 arcsec aperture diameter)
76 : gHlCorSMjRadAs; E; Seeing corrected half-light, semi-major axis in G band
77 : gGausig; E; RMS of axes of ellipse fit in G

78 : gEll; E; 1-b/a, where a/b=semi-major/minor axes in G
79 : gPA; E; ellipse fit celestial orientation in G
80 : gErrBits; J; processing warning/error bitwise flags in G
81 : gAverageConf; E; average confidence in 2 arcsec diameter default aperture (aper3) G
82 : gClass; I; discrete image classification flag in G
83 : gClassStat; E; N(0,1) stellarness-of-profile statistic in G
84 : gppErrBits; J; additional WFAU post-processing error bits in G
85 : gSeqNum; J; the running number of the G detection
86 : gXi; E; Offset of G detection from master position (+east/-west)
87 : gEta; E; Offset of G detection from master position (+north/-south)
88 : rMjd; D; The mean Modified Julian Day of each detection
89 : rPetroMag; E; Extended source R mag (Petrosian)
90 : rPetroMagErr; E; Error in extended source R mag (Petrosian)
91 : rAperMag3; E; Default point source R aperture corrected mag (2.0 arcsec aperture diameter)
92 : rAperMag3Err; E; Error in default point/extended source R mag (2.0 arcsec aperture diameter)
93 : rAperMag4; E; Point source R aperture corrected mag (2.8 arcsec aperture diameter)
94 : rAperMag4Err; E; Error in point/extended source R mag (2.8 arcsec aperture diameter)
95 : rAperMag6; E; Point source R aperture corrected mag (5.7 arcsec aperture diameter)
96 : rAperMag6Err; E; Error in point/extended source R mag (5.7 arcsec aperture diameter)
97 : rAperMagNoAperCorr3; E; Default extended source R aperture mag (2.0 arcsec aperture diameter)
98 : rAperMagNoAperCorr4; E; Extended source R aperture mag (2.8 arcsec aperture diameter)
99 : rAperMagNoAperCorr6; E; Extended source R aperture mag (5.7 arcsec aperture diameter)
100 : rHlCorSMjRadAs; E; Seeing corrected half-light, semi-major axis in R band
101 : rGausig; E; RMS of axes of ellipse fit in R
102 : rEll; E; 1-b/a, where a/b=semi-major/minor axes in R
103 : rPA; E; ellipse fit celestial orientation in R
104 : rErrBits; J; processing warning/error bitwise flags in R
105 : rAverageConf; E; average confidence in 2 arcsec diameter default aperture (aper3) R
106 : rClass; I; discrete image classification flag in R
107 : rClassStat; E; N(0,1) stellarness-of-profile statistic in R
108 : rppErrBits; J; additional WFAU post-processing error bits in R
109 : rSeqNum; J; the running number of the R detection
110 : rXi; E; Offset of R detection from master position (+east/-west)
111 : rEta; E; Offset of R detection from master position (+north/-south)
112 : iMjd; D; The mean Modified Julian Day of each detection
113 : iPetroMag; E; Extended source I mag (Petrosian)
114 : iPetroMagErr; E; Error in extended source I mag (Petrosian)
115 : iAperMag3; E; Default point source I aperture corrected mag (2.0 arcsec aperture diameter)
116 : iAperMag3Err; E; Error in default point/extended source I mag (2.0 arcsec aperture diameter)
117 : iAperMag4; E; Point source I aperture corrected mag (2.8 arcsec aperture diameter)
118 : iAperMag4Err; E; Error in point/extended source I mag (2.8 arcsec aperture diameter)
119 : iAperMag6; E; Point source I aperture corrected mag (5.7 arcsec aperture diameter)
120 : iAperMag6Err; E; Error in point/extended source I mag (5.7 arcsec aperture diameter)
121 : iAperMagNoAperCorr3; E; Default extended source I aperture mag (2.0 arcsec aperture diameter)
122 : iAperMagNoAperCorr4; E; Extended source I aperture mag (2.8 arcsec aperture diameter)
123 : iAperMagNoAperCorr6; E; Extended source I aperture mag (5.7 arcsec aperture diameter)
124 : iHlCorSMjRadAs; E; Seeing corrected half-light, semi-major axis in I band
125 : iGausig; E; RMS of axes of ellipse fit in I
126 : iEll; E; 1-b/a, where a/b=semi-major/minor axes in I
127 : iPA; E; ellipse fit celestial orientation in I
128 : iErrBits; J; processing warning/error bitwise flags in I
129 : iAverageConf; E; average confidence in 2 arcsec diameter default aperture (aper3) I
130 : iClass; I; discrete image classification flag in I
131 : iClassStat; E; N(0,1) stellarness-of-profile statistic in I
132 : ippErrBits; J; additional WFAU post-processing error bits in I

133 : iSeqNum; J; the running number of the I detection
134 : iXi; E; Offset of I detection from master position (+east/-west)
135 : iEta; E; Offset of I detection from master position (+north/-south)
136 : zMjd; D; The mean Modified Julian Day of each detection
137 : zPetroMag; E; Extended source Z mag (Petrosian)
138 : zPetroMagErr; E; Error in extended source Z mag (Petrosian)
139 : zAperMag3; E; Default point source Z aperture corrected mag (2.0 arcsec aperture diameter)
140 : zAperMag3Err; E; Error in default point/extended source Z mag (2.0 arcsec aperture diameter)
141 : zAperMag4; E; Point source Z aperture corrected mag (2.8 arcsec aperture diameter)
142 : zAperMag4Err; E; Error in point/extended source Z mag (2.8 arcsec aperture diameter)
143 : zAperMag6; E; Point source Z aperture corrected mag (5.7 arcsec aperture diameter)
144 : zAperMag6Err; E; Error in point/extended source Z mag (5.7 arcsec aperture diameter)
145 : zAperMagNoAperCorr3; E; Default extended source Z aperture mag (2.0 arcsec aperture diameter)
146 : zAperMagNoAperCorr4; E; Extended source Z aperture mag (2.8 arcsec aperture diameter)
147 : zAperMagNoAperCorr6; E; Extended source Z aperture mag (5.7 arcsec aperture diameter)
148 : zHlCorSMjRadAs; E; Seeing corrected half-light, semi-major axis in Z band
149 : zGausig; E; RMS of axes of ellipse fit in Z
150 : zEll; E; 1-b/a, where a/b=semi-major/minor axes in Z
151 : zPA; E; ellipse fit celestial orientation in Z
152 : zErrBits; J; processing warning/error bitwise flags in Z
153 : zAverageConf; E; average confidence in 2 arcsec diameter default aperture (aper3) Z
154 : zClass; I; discrete image classification flag in Z
155 : zClassStat; E; N(0,1) stellarness-of-profile statistic in Z
156 : zppErrBits; J; additional WFAU post-processing error bits in Z
157 : zSeqNum; J; the running number of the Z detection
158 : zXi; E; Offset of Z detection from master position (+east/-west)
159 : zEta; E; Offset of Z detection from master position (+north/-south)
160 : PRIMARY_SOURCE; B; Primary source 1; secondary source 0